Light Metals 2012 *Edited by: Carlos E. Suarez*
TMS (The Minerals, Metals & Materials Society), 2012

PROPERTIES AND PRODUCTION CONDITIONS AFFECTING CRACK FORMATION AND PROPAGATION IN CARBON ANODES

O. E. Frosta[1,2], A. P. Ratvik[1], H. A. Øye[1]
[1.] Department of Materials Science and Engineering, Norwegian University of Science and Technology (NTNU)
N-7491 Trondheim, Norway
[2.] Hydro Aluminium ASA, Primary Metal Technology, N-6881 Årdalstangen, Norway

Keywords: Carbon anodes, Modelling, Anode Cracking, Mechanical strength

Abstract

The objective of the present work is to achieve a better understanding of anode thermal shock fracture in the early stage after an anode change in the electrolysis cell. In order to show the mechanisms leading to anode fracture and crack propagation, a thermo-mechanical model of the thermal shock experienced by an anode when it is positioned in the pot was developed. The model allows calculation of stresses and strains within the anode, as function of time. The time interval of the modelling lasts for 1 hour after the anode change.

Baked anodes are inhomogeneous and anisotropic due to the raw materials and production process. Core samples from industrial scale anodes were analysed and the results provided gradient plots of physical and mechanical properties. The results were used as input to the model and together with a set of boundary conditions, the thermal shock resistance was calculated.

The highest main tensile stress occurred 1 hour after the anode is immersed in the cell. The stress seems then to level out and decrease. The stress calculated is at a level where cracks may be initiated, matching the tensile strength tests.

Introduction and experimental

The anode is not homogeneous when it goes into the pot due to production parameters. The main reason is the forming stage of the green block. After the mixing stage in the paste plant, the material is fed to weighing hoppers, usually one on each long side of the vibration mould. When the hoppers are filled to a given level, the input feed stops and the mixed material is filled into the mould. Due to the physical properties of the paste and the construction of this part of the production line, there is often an uneven filling in the mould. The combination with high filling in the long sides, low filling in the centre and the chamfered top causes less energy to be transferred into the middle of the anode. These elements will contribute to make the anode body inhomogeneous by introducing material property gradients.
All input in the study is based on sample tests of industrial anodes with the dimensions 1600·700·600 (L·W·H in mm).

There are three different approaches to how the anodes were analyzed;

1) Core samples drilled out for a number of physical and element analyses.

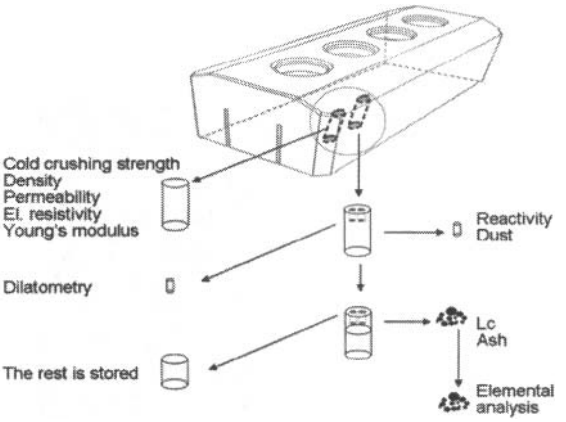

Figure 1. Core sample analysis of anode blocks [1].

2) Rectangular blocks machined out for measuring the fracture toughness in a three point bending test, in total 32 specimens [2]. A quarter of an anode was used in this test.

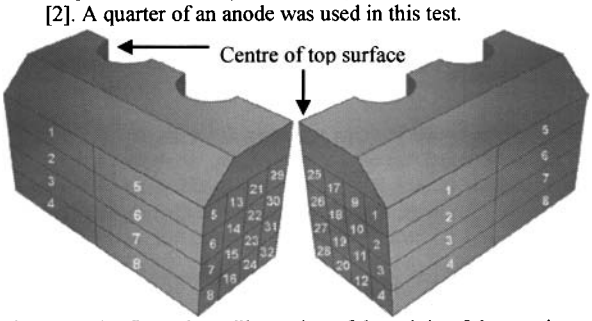

Figure 2. The figure is an illustration of the origin of the specimen in the experimental study, corresponding to their specimen number. The quarter anode is shown from two angles in order to show the location of the different specimens.

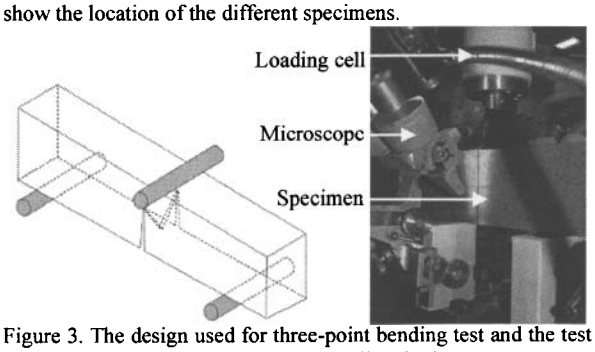

Figure 3. The design used for three-point bending test and the test assembly with anode sample, loading cell and microscope.

3) Machined core samples for tensile testing. 20 cores were drilled out from correspondingly three sections (in total 60 specimens). Tensile tests were conducted at 20, 200 and 400 °C [3].

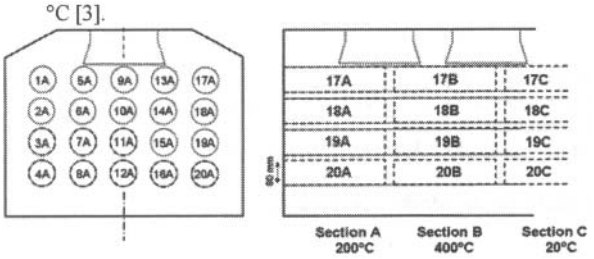

Figure 4. The figures illustrate the sampling pattern of the circular core samples from the anode.

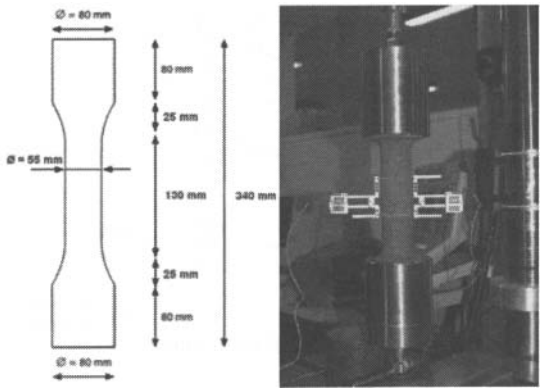

Figure 5. The design used for tensile testing and the load train assembly with anode sample, loading cell and extensiometers.

The modelling is based on the FEM-program ANSYS. The study covers the first hour following an anode change.

Spreadsheets where position accompanied with physical material properties through the anode were made. Analysis of numerous samples from various positions in the anode made the basis for these data. This made it possible to simulate the inhomogeneity of the anode and the data from the spreadsheets was used as input to the model.

Results and discussion

Fracture toughness

The critical stress intensity factor, K_{Ic}, is determined from the knowledge of the dimensions of the test specimen and the data retrieved from the force versus displacement record of the fracture test. The fracture toughness, K_{Ic}, is given by Equation 1.

$$K_{Ic} = \frac{F_Q S_p}{B W^{1.5}} f\left(\frac{a_0}{W}\right) \quad (1)$$

where

$$f\left(\frac{a_0}{W}\right) = \frac{3\left(\frac{a_0}{W}\right)^{0.5}\left[1.99 - \left(\frac{a_0}{W}\right)\left(1-\frac{a_0}{W}\right)\left(2.15 - \frac{3.93 a_0}{W} + \frac{2.7 a_0^2}{W^2}\right)\right]}{2\left(1+\frac{2a_0}{W}\right)\left(1-\frac{a_0}{W}\right)^{1.5}} \quad (2)$$

and

F_Q	Maximum value of the applied force between the two unloadings	[N]
S_p	Span between the outer loading points	[mm]
B	Specimen thickness	[mm]
W	Specimen height	[mm]
a_0	Average measured crack length	[mm]

The fracture toughness is assumed to be a constant in general fracture mechanics. However, from the derived K_{Ic} values, it can be seen that the fracture toughness increases with the crack size. The increase in the fracture toughness indicates that there is a limit of validity.

There is a tendency that the K_{Ic} values start to increase in the area where the crack length is close to 20 mm. An explanation may be that Equation 1 no longer is valid for the estimation of K_{Ic} at these crack lengths. The increased K_{Ic} could also be due to changing conditions at the crack tip.

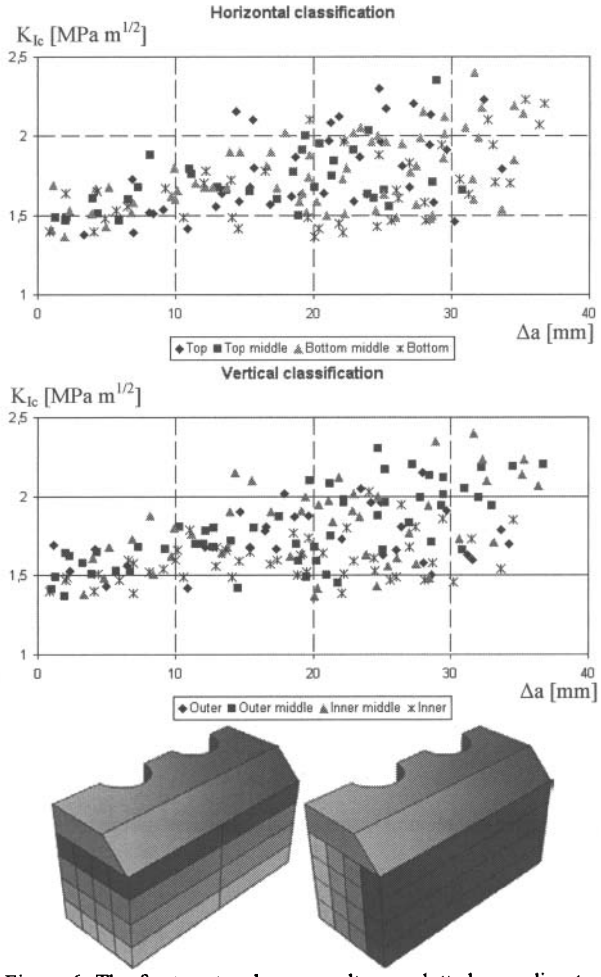

Figure 6. The fracture toughness results are plotted according to horizontal and vertical layers. The figures show the layering of the quarter anode (horizontal left, vertical right).

Table I. The average fracture toughness values for vertical and horizontal classification are presented in the table. The classification is described in Figure 6.

Vertical classification	Outer	Outer middle	Inner middle	Inner
Average fracture toughness K_{Ic} [MPa $m^{1/2}$]	1.74	1.79	1.81	1.60
Horizontal classification	Top	Top middle	Bottom middle	Bottom
Average fracture toughness K_{Ic} [MPa $m^{1/2}$]	1.78	1.70	1.77	1.68

As seen from Figure 6 and Table I the fracture toughness is apparently independent of sample direction.

A possible explanation for any deviating results may be referred to a segregation of the paste in the mould. A coarser granulometry at the lower parts of the anode surface is to some degree difficult to avoid. Coarser paste composition, either consisting of baked scrap/butts material or coke grains, can give deflecting results of fracture toughness in both directions in such tests.

In order to interpret the fracture toughness results statistically, the Weibull distribution is applied. Several fracture toughness values were retrieved per specimen. Each value is presented according to the corresponding crack length. In the statistical analysis conducted, the crack length is no longer used as a variable as a value independent of the crack size is used. One specimen thus holds several different values. Two maximum values of the critical crack length were chosen to be analysed, 10 and 15 mm respectively. These crack lengths are within what can be the validation limit of Equation 2.

Figure 7 illustrates the distribution density for both a_{crit} = 10 mm and a_{crit} = 15 mm. The distribution density for a_{crit} = 10 mm exhibit a more narrow curve, compared to the distribution density of a_{crit} = 15 mm. A survival probability of 95 % for the cracks < 15 mm results in a fracture toughness of approximately 1.3 MPa $m^{1/2}$. This is a quite low estimation as most of the result are within the range of 1.5 – 1.6 MPa $m^{1/2}$.

Table II. Weibull parameters for the fracture toughness results.

K_{Ic} results	a_{crit} < 10 mm	a_{crit} < 15 mm
Mean	1.540	1.595
Standard deviation	0.150	0.185
$\frac{1}{\sigma_0^m}$	1.68	1.60
m	10.30	12.23

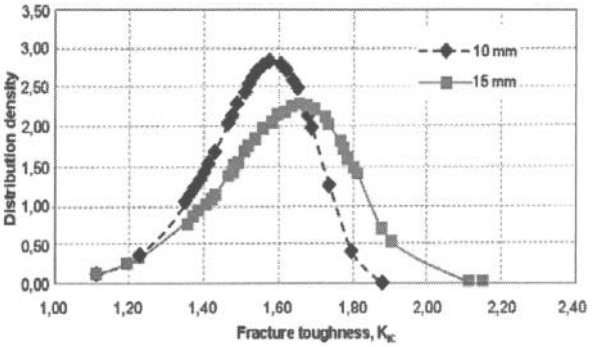

Figure 7. All the fracture toughness values are represented by a Weibull distribution where 10 mm and 15 mm are chosen as the maximum critical crack lengths.

In the statistical analysis of a_{crit} = 15 mm, twenty-six specimens and sixty-seven K_{Ic} values were used. For a_{crit} = 10 mm twenty-four test specimens had forty-one observed K_{Ic} values.

Tensile testing

To determine the Young's modulus and tensile strength of the anode, tension tests were conducted at three temperature levels, 20 °C, 200 °C and 400 °C. Figure 5 is a schematic drawing of the apparatus used in tension tests.

Table III. Weibull distribution parameters for the tensile testing. Results are displayed in Figure 8.

Parameter	Temp [°C]	Stress [MPa]	Strain [%]	Young's Modulus [MPa]
$\frac{1}{\sigma_0^m}$	20	6.380	0.0779	9350
	200	6.372	0.0892	8356
	400	8.043	0.1117	8965
m	20	15.641	10.252	15.700
	200	6.223	4.865	7.735
	400	14.528	6.086	8.064
mean μ [MPa]	20	6.169	0.07422	9042
	200	5.923	0.08181	7838
	400	7.759	0.10373	8446
variance σ^2	20	0.235	0.761e-04	0.501e06
	200	1.232	3.692e-04	1.574e06
	400	0.428	3.394e-04	1.547e06

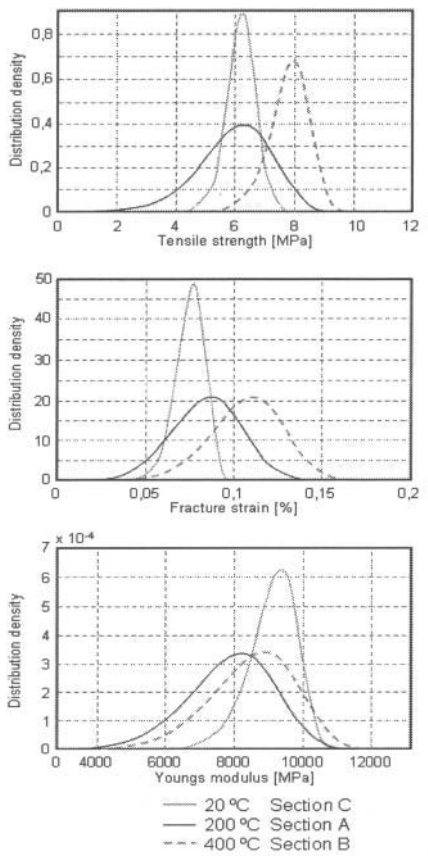

Figure 8. The results from the tensile tests plotted with Weibull distribution.

Given survival rates of 50 and 95 %, the tensile strength in MPa at 20, 200 and 400 °C are as follows;

Survival rate	20 °C	200 °C	400 °C
50 %	6.25	6.04	7.88
95 %	5.26	3.99	6.54

Due to the relatively large scatter in results at 200 °C, the survival rate is rather low. This scatter is more likely to be related to placement (inhomogeneity) than temperature.

Given survival rates of 50 and 95 %, the critical strain in % at 20, 200 and 400 °C are as follows;

Survival rate	20 °C	200 °C	400 °C
50 %	0.0747	0.0828	0.1051
95 %	0.0586	0.0485	0.0687

By using the average results at each temperature level, the tensile stress increased by 26 %, the tensile strain by 42 %, and the Young's modulus reduced by 7 % when comparing results at 20 °C and 400 °C.

Both the tensile strength and the Young's modulus seem to correlate with the density of the anode whereas the critical strain shows no correlation.

A number of voids and cracks were found in the anode material. The voids may arise from either the production process, or they can be inherent in the raw material of the anode. Cracks and flaws within the anode explain some unpredictable failure of the tests from the anode. The failure of the carbon material originates from defects. The defects scatter in size and this may be the main factor causing relatively large scatter in the results.

Previous tests have shown a large difference in strength according to the direction of the specimen in the anode. Nerland [4] discovered that the Young's modulus were 10 % lower in the direction parallel to the vibration direction compared to the normal direction. The compressive strength had a 21 % lower strength in the parallel compared to the normal direction. These were values found in laboratory scale anodes, but the same tendency has been observed in large scale anodes (an-isotropy of 10 – 20 %) [5]. All specimens used in the mechanical tests are parallel to the vibration direction.

Modelling

The results from the physical and mechanical testing were transferred to the FEM-program ANSYS. Stresses arising within the anode during the first hour after immersed in to the cell were calculated. Three different profiles of the gradients through the anode are presented in Case 1 – Case 3 (Figure 9). All profiles are symmetric about a vertical plane running longitudinal along the stub holes and about a vertical plane transversal through the middle of the centre stub holes.

The three profiles hold parameters that can be seen in regular industrial scale anodes, but the gradients are made in such a way that they represent both the tray shaped profile, the homogeneous profile, and the hill shaped profile. The physical composition of the anode used in modelling is illustrated by a contour map showing the density gradients in a horizontal layer at 480 mm height. The contour lines of the map are given by thicker lines. The maps are relatively exaggerated in terms of gradient profile in order to emphasise inhomogeneity. The contour lines are closer at the upper part of the anode compared to the lower part. The gradients are, hence, smaller going towards the lower parts of the anode.

Case 1 (tray shaped) is commonly observed in production. Case 2 (homogeneous) is what to be expected as ideal. Case 3 (hill shaped) is investigated in order to obtain stress calculations from both "sides" of the ideal case.

Case 1: Tray shaped profile (density 1.576 – 1.606 kg/dm^3)

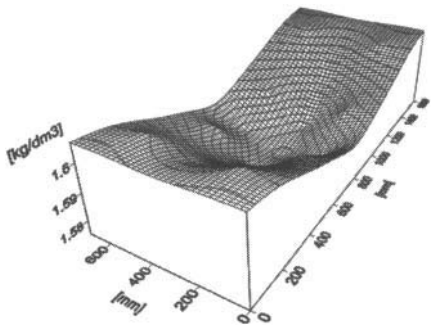

Case 2: Homogeneous profile (density 1.59 kg/dm^3)

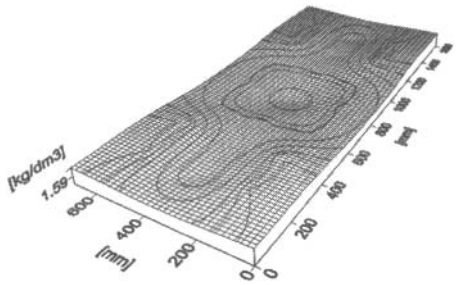

Case 3: Hill shaped profile (density 1.574 – 1.604 kg/dm)

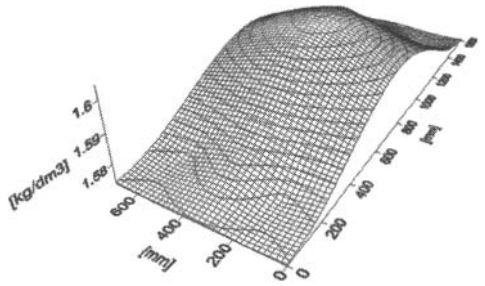

Figure 9. Three different cases of gradients profiles of anodes are modelled. These three plots show density gradients through a horizontal cross section at 480 mm height of the anodes used in the model.

Corner cracking

As a fracture criterion of corner cracking, a concept of equivalent tensile stress is used. The elaboration of such a criterion has been a subject of a thesis on concrete [6]. The equivalent tensile stress is defined as;

$$\sigma_{eq} = \sqrt{\sigma_x^{\,2} + \sigma_y^{\,2} + \sigma_z^{\,2}} \qquad (3)$$

where

$\sigma_i = \sigma_i$ if $\sigma_i > 0$

$\sigma_i = 0$ if $\sigma_i \le 0$

For a given element, the equivalent tensile stress is thus the quadratic root of the quadratic sum of the stresses due to tensile load only.

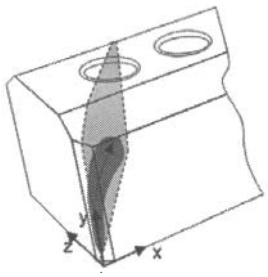

Figure 10. A vertical plan running through the corner of the anode and 42 ° on the x-direction in the xz-plane is shown in the figure. Tensile stress calculations in this plane are plotted in Figure 11. The dark grey "zone" indicates the development and direction of the main tensile stress in the corner area (starting at the corner and runs along the plane in a hyperbolic pattern, indicated by the thin arrow).

Table IV. Position of the tensile stress plots in Figure 11. The node positions are within the greyish plane seen in Figure 10.

Position [cm] / Node	x	z	y
1	6	5.4	6.5
2	7	6.3	8
3	10	9	10
4	14.2	12.78	12
5	16	14.4	14

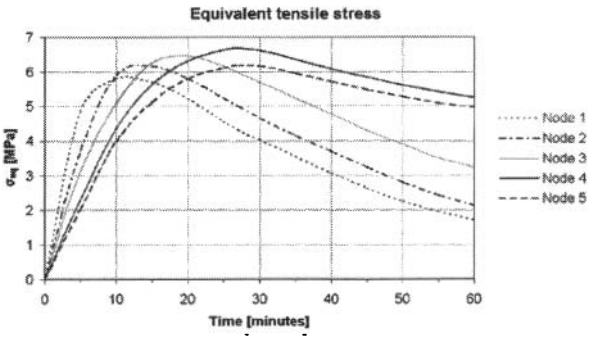

Figure 11. The equivalent tensile stress development in the corner area versus time at positions given in Table IV is plotted in the graph.

The tensile stress runs from the lower corner towards the centre of the anode. In the corner the main tensile force works along a hyperbolic shaped line running from the lower corner towards the centre of the anode. A crack will run from the point it was initiated and perpendicular to the main tensile stress, i.e. normal to this hyperbolic shaped arrow in Figure 10. The equivalent tensile stress reaches a maximum after approximately 27 minutes (see Figure 11). However, after five minutes the stress is at a level where cracking may take place. This indicates that there is a risk of corner fracture in the time interval between approximately five and thirty minutes. The results from the calculations, both in time and direction, coincide with how corner breakage in real operation occurs.

As the material properties within the three gradient profiles are approximately equal in the area where corner breakage normally occurs, there is no difference in the equivalent stress derived.

Vertical cracking

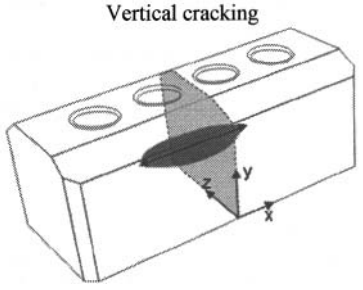

Figure 12. A vertical plane running transversal through the middle of the anode is shown in the figure (in the yz-plane). The maximum tensile stresses in the horizontal direction perpendicular to this plane are plotted in Figure 13. The dark grey "zone" indicates the direction and placing of the main tensile stress in the middle of the anode.

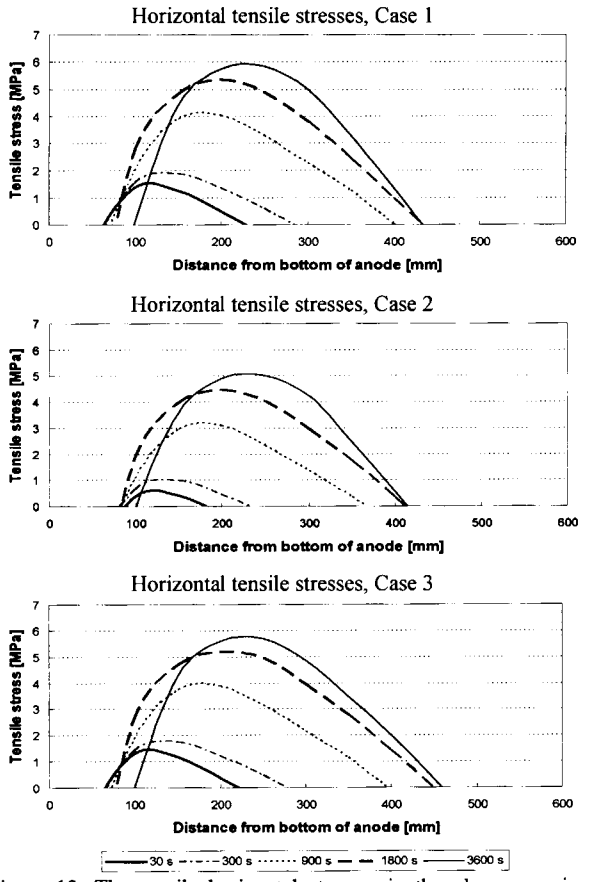

Figure 13. The tensile horizontal stresses in the plane seen in Figure 12 are plotted as function of height of anode for each of the three cases (see Figure 9). Each line represents the stress level at a certain point in time after anode change. The highest stresses for each case are correspondingly 5.85, 5.03 and 5.70 MPa.

When an anode is inserted to the cell, expansion of the hot surface layer creates tension in the cold carbon immediately inside. Conversely, the surface is in compression due to restraints by the interior carbon. As heat conducts into the anode, the layer in tension moves progressively further inward and upward.

The horizontal tensile stresses perpendicular to the plane shown in Figure 12 are plotted in Figure 13. The horizontal stresses increase relatively fast within the first 30 minutes and then more slowly. It is in the mid section of the anode the highest stresses arise, at approximately 250 mm height. The main tensile strength is horizontal, referring to the case of corner cracking where the main tensile stress could be found along a hyperbolic shaped curve running from the lower corner towards a horizontal asymptote at the centre of the anode. The stresses reach the highest level ca 1 hour after anode change. The stress level seems then to level out and to decrease. The risk of vertical cracking starts approximately after 25 minutes and increases with time until one hour.

Case 2, the homogeneous anode, is most favourable dealing with thermal shock properties. With a 14 % lower tensile stress compared to the "normal case" (1), the probability of any crack initiation or propagation is reduced.

Case 3 (hill shaped) has a somewhat smaller stress arising compared to 1. A possible explanation may be that a higher thermal conductivity gives a more positive effect on the stress development than a lower Young's modulus. There is also an indication of the tensile stresses moving faster upwards in the anode in case 3.

Conclusions

Mechanical tests of industrial scale anodes have been performed. The fracture toughness, based on the critical stress intensity factor K_{Ic}, was found to be 1.3 MPa $m^{1/2}$ with a survival rate of 95 %.

Tensile data with a survival probability of 95 %;

	20 °C	200 °C	400 °C
Tensile strength [MPa]	5.26	3.99	6.54
Critical Strain [%]	0.0586	0.0485	0.0687

Both the tensile strength and the Young's modulus seem to correlate with the density of the anode whereas the critical strain and the fracture toughness show no correlation.

The highest main tensile stress occurs 1 hour after the anode is immersed into the cell. The stress seems then to level out and to decrease. The stress calculated and shown in Figure 13 is at a level where cracks may be initiated, matching the tensile strength tests. However, fracture toughening mechanisms as micro cracking and branching do reduce the failure rate of anode cracking.

When comparing three anodes with different physical gradients a homogeneous anode is, as expected, preferable when it comes to thermal shock resistance.

References

1 ISO and DIN standards, and Internal Standard, Hydro Aluminium Årdal.

2 L. Eliassen, Characterization of the mechanical properties of carbon anode materials, Project report, Department of Structural Engineering, Norwegian University of Science and Technology (NTNU), (2006).

3 L. Eliassen, Characterization of the mechanical properties of carbon anode materials, Norwegian University of Science and Technology (NTNU), Master Thesis (2007).

4 A.M. Nerland, Thermal shock resistance of anode carbon for aluminium electrolysis, Ph.D thesis, Norwegian University of Science and Technology (1994).

5 J. P. Schneider and B. Coste, Thermal shock of anodes: influence of raw materials and manufacturing parameters, *Light Metals (Warrendale, PA, United States)* (1993), 611-619.

6 J. Mazars, Application de la mecanique de'lendommagement au comportement non lineaire et a la rupture du beton de structure, These de doctorat, Universite Pierre et Marie Curie Paris VI (1984)